Accounting for spectral bandwidth broadening due to self-phase modulation in measurements of laser pulse transmission through a dense plasma

Contact: ewan.dolier.2015@uni.strath.ac.uk

E. J. Dolier, R. Wilson, T. P. Frazer, J. Goodman, A. Lofrese, A. Horne, M. King, R. J. Gray and P. McKenna
SUPA Department of Physics, University of Strathclyde, G4 0NG, United Kingdom

T. Dzelzainis and D. Neely
Central Laser Facility, STFC Rutherford Appleton Laboratory, Harwell Campus, Didcot OX11 0QX, United Kingdom

Abstract

A method has been developed to characterise the fraction of laser energy transmitted through an initially overdense plasma whilst accounting for broadening in the transmitted pulse spectrum. As such, this method accounts for the effect of self-phase modulation which may occur as an intense pulse propagates through beam-line optics before being detected.

1 Introduction

At high intensities (>10^{18} Wcm^{-2}), some fraction of an incident laser pulse can propagate through a nanometre scale target due to relativistic self-induced transparency (RSIT) [1–3]. The onset of RSIT has been shown to enhance the maximum energy of ions in a hybrid acceleration scheme [4], and to result in ion beams of relatively narrow energy spread [5]. Such a scheme has also been proposed as a means to control the collective response of electrons and ions accelerated during a laser-plasma interaction [6, 7]. The fraction of laser energy transmitted during the interaction is indicative of RSIT onset time relative to the peak laser intensity, and gives an indication of whether these mechanisms will occur. In this report, a method for quantifying the fraction of laser pulse transmission through an initially overdense plasma is detailed and applied to results from a recent Astra-Gemini (TA3) experimental campaign. On analysis, measurements of the transmitted pulse spectrum demonstrate broadening relative to the initial laser spectrum, indicating the pulse had undergone self-phase modulation (SPM) whilst propagating through optics after the target. Measurements of the transmitted spatial-intensity distribution, often used to quantify the fraction of laser pulse transmission, were made using a CCD camera fitted with an interference filter so as to only measure light at the fundamental laser wavelength. As a result, the camera was unable to quantify the entirety of the broadened transmitted light spectrum. By combining spectral and spatial measurements of the transmitted light, a comprehensive technique has been developed to characterise the fraction of incident energy transmitted during a laser-plasma interaction whilst accounting for SPM which may occur before the measurement is made.

2 Experimental methodology

Using the Astra-Gemini facility (TA3), linear-p polarised pulses with a central wavelength, λ_L, of 790 nm, full width at half maximum (FWHM) bandwidth of $\sim$ 30 nm, a duration, τ_L, of 40 fs (FWHM) and energy, E_L, of $\sim$ 5 J, were focused to $\sim$ 3 μm (FWHM) using a f/2 OAP, as shown in Fig. 1 (a). Aluminium targets with thickness ranging from 10-113 nm were irradiated at 0° with respect to target normal and light transmitted through the target was re-collimated using another f/2 OAP and directed out of the chamber using two low reflectivity ($\sim$ 4% at 800 nm) wedged mirrors so that the polarisation of transmitted light could be characterised using a Stokes polarimeter [8].

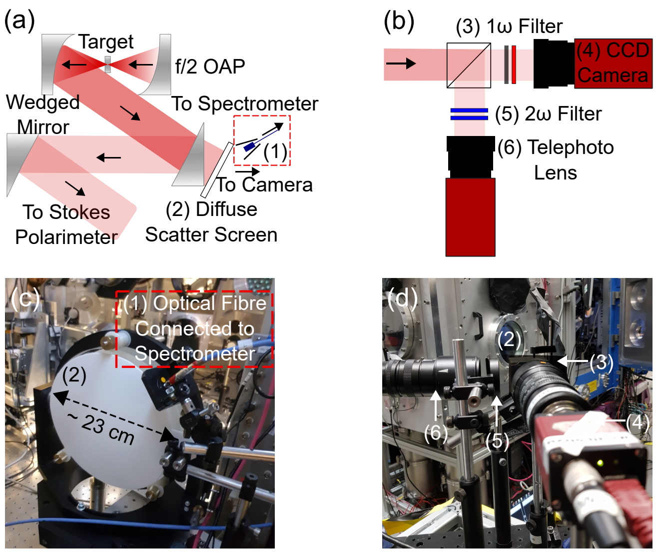

Figure 1: (a) Illustration of the experimental setup where a high intensity pulse is focused onto a thin aluminium target. Light transmitted through the target is re-collimated and diffusely scattered by a PTFE screen for (b) imaging using CCD cameras. Photos of the diffuse scatter screen and the filtered camera setup are shown in (c) and (d) respectively.

Using a PTFE screen, transmitted light was diffusely scattered and imaged using CCD cameras situated outside the chamber (as shown in Fig. 1 (b) and (d)). To collect light at only the fundamental (1ω) and second harmonic (2ω) wavelength, interference filters with a central wavelength of 800 nm and 400 nm were placed in front of the respective cameras as shown in Fig. 1 (b). The spectral bandwidth of these filters, measured at FWHM, is 40 nm, and so transmitted light with wavelength outside this range will be strongly attenuated and essentially undetectable to the camera. An optical fibre mounted behind the scatter screen was coupled to a spectrometer as shown in Fig. 1 (a) and (c) to collect a small cross-section of transmitted light for spectral analysis.

3 Measuring transmitted energy using a filtered camera diagnostic

As shown in Fig. 1 (a), several diagnostics were used to analyse light transmitted through ultra-thin aluminium targets by summing the number of 'counts' across each pixel of a detector. However, for these measurements to be of use, a 'signal-energy' calibration must first be generated from a series of shots with no target in the beamline. The transmitted light signal was measured for each of these shots using the filtered 1ω camera and increases linearly with increasing incident laser energy (black data in Fig. 2) as expected [9]. By taking the gradient of a linear fit to this data, the summed signal measured after transmission through a target can be converted into energy and compared to the incident laser energy. As such, the fraction of light transmitted through a target when RSIT occurs can be characterised.

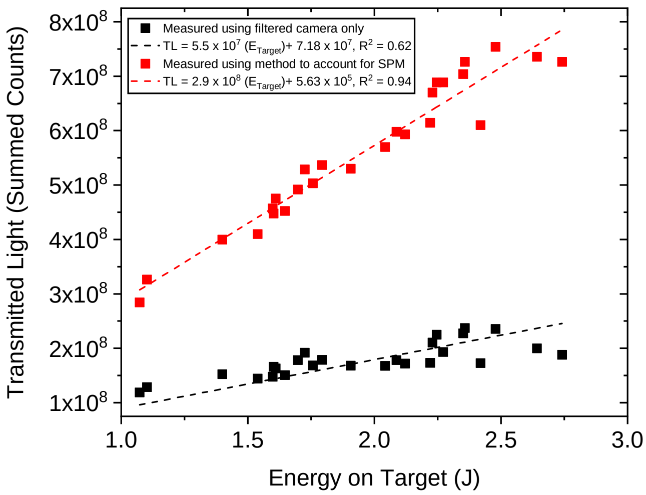

Figure 2: Transmitted light measurements for no target shots with varying incident laser energy. Transmitted light was measured using the 1ω filtered camera alone (black) and by combining filtered camera and spectrometer measurements to account for SPM-induced spectral broadening (red).

4 Spectral broadening of the transmitted pulse

Complimentary spectral measurements of the transmitted light displayed broadened spectra compared to that of the incident laser pulse which has a bandwidth, $\triangle\lambda$, of $\sim$ 30 nm (FWHM). As the camera was fitted with an interference filter of $\triangle\lambda = (40 \pm 8)$ nm, a significant proportion (50% - 80%) of light went undetected by the camera as shown in Fig. 3.

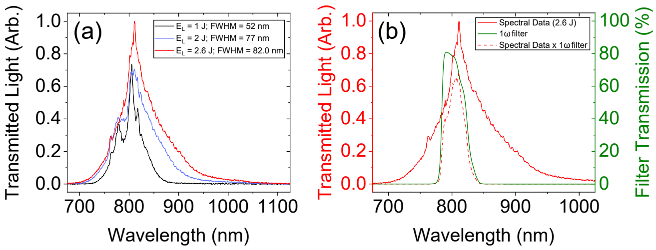

Figure 3: (a) Transmitted light spectra for several no target shots display increased bandwidth (FWHM) with increasing incident laser energy, suggesting SPM-induced broadening. (b) An example transmitted light spectrum (solid red) is shown for a no target shot, alongside the transmission curve of the $\triangle\lambda = 40$ nm interference filter placed in front of the CCD camera (green). Spectral measurements were multiplied by this transmission curve (dashed red), indicating the proportion of transmitted light which has gone undetected by the filtered camera.

Such spectral broadening results in a poor linear fit ($R^2 = 0.62$) to the calibration data presented in Fig. 2, where transmitted light was measured using the filtered camera alone. Ultimately, this leads to an incorrect method for measuring the fraction of energy transmitted through a target. The observed spectral broadening occurs as the transmitted pulse propagates through a 3 cm thick fused silica wedged mirror as shown in Fig. 1 (a), at which point the beam has been re-collimated to a diameter of $\sim$ 15 cm. On propagation through the mirror, there is an intensity dependent modulation to the pulse spectrum as described by the B-integral [10];

$$B = \frac{2\pi}{\lambda_L} \int n_2 I_L(z) dz \tag{1}$$

where n_2 is the nonlinear component of the refractive index, $n = n_0 + n_2 I_L(z)$. For fused silica, $n_2 = 2.48$ x 10^{-16} cm^2W^{-1} at 800 nm [11], resulting in a B-integral ranging from 7 to 19 for the example no target shots presented in Fig. 3. Self-phase modulation is generally expected when the B-integral is >3 [10] and so, the spectral broadening observed throughout the experiment can be attributed to SPM as the pulse propagates through the low reflectivity wedged mirror. In future, if a similar experimental setup is employed, the transmitted light spectrum will be characterised before the fused silica wedge to confirm this conclusion.

5 Measuring transmitted energy whilst accounting for self-phase modulation

As discussed, transmitted energy measurements made using the 1ω filtered camera alone will not account for SPM induced spectral broadening due to the bandwidth of the interference filter. To account for SPM, the signal measured by the optical spectrometer was first multiplied by the spectral transmission curve of the interference filter (green in Fig. 3 (a)). The spectral signal was then summed before and after this filtering, with the resultant ratio conveying the proportion of transmitted light which the camera is unable to detect. Signal captured on the camera was then summed and multiplied by this ratio, effectively replicating the signal which would have been captured by the camera had there been no filter in place. Additionally, by using the spectrometer to scale the camera measurements in this way, signal which typically goes undetected as a result of the cameras quantum efficiency is accounted for.

Using this method, the relationship between the measured transmitted light signal and the incident laser energy is well approximated by a linear fit ($R^2 = 0.94$) over a series of no target shots as shown in Fig. 2. This is not the case when measuring the transmitted light signal using the filtered camera alone ($R^2 = 0.62$).

Using the spectral and spatial measurements together, signal-energy calibrations were calculated and employed to characterise the degree of transparency when irradiating aluminium foil targets of varying thickness.

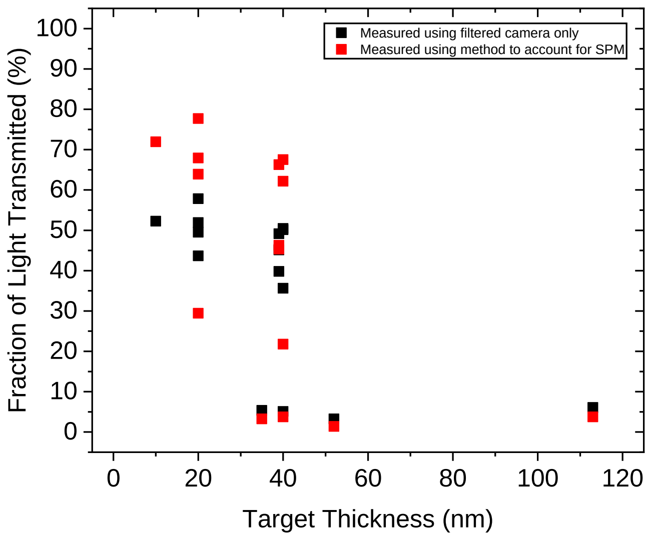

Figure 4: Aluminium targets of varying thickness were irradiated using linear p-polarised pulses of $E_L \sim 5$ J and $\tau_L \sim 40$ fs. Light transmitted through the target was detected and converted to an energy measurement using both the filtered camera method and the method developed to account for SPM.

As a result, the fraction of energy transmitted through a target when RSIT occurs can be measured whilst fully accounting for SPM which occurs as the light propagates through optics before detection.

6 Conclusion

A technique has been developed to measure light transmitted through a nanometre scale target under conditions where the intensity is sufficient for self-phase modulation to occur before the light is detected. Using both spectral and spatial measurements of the transmitted light, SPM induced spectral broadening of the transmitted pulse is fully accounted for. As a result, this diagnostic technique can be applied to a wide range of experimental conditions and setups to accurately measure the fraction of incident laser energy transmitted through a target when RSIT occurs.

References

[1] P. Kaw and J. Dawson. Relativistic nonlinear propagation of laser beams in cold overdense plasmas. *The Physics of Fluids*, 13(2):472–481, 1970.

[2] V. A. Vshivkov et al. Nonlinear electrodynamics of the interaction of ultra-intense laser pulses with a thin foil. *Physics of Plasmas*, 5(7):2727–2741, 1998.

[3] S. Palaniyappan et al. Dynamics of relativistic transparency and optical shuttering in expanding overdense plasmas. *Nature Physics*, 8(10):763–769, 2012.

[4] A. Higginson et al. Near-100 mev protons via a laser-driven transparency-enhanced hybrid acceleration scheme. *Nature communications*, 9(1):1–9, 2018.

[5] S. Palaniyappan et al. Efficient quasi-monoenergetic ion beams from laser-driven relativistic plasmas. *Nature communications*, 6(1):1–12, 2015.

[6] B. Gonzalez-Izquierdo et al. Optically controlled dense current structures driven by relativistic plasma aperture-induced diffraction. *Nature Physics*, 12(5):505–512, 2016.

[7] B. Gonzalez-Izquierdo et al. Towards optical polarization control of laser-driven proton acceleration in foils undergoing relativistic transparency. *Nature communications*, 7(1):1–10, 2016.

[8] M. J. Duff et al. High order mode structure of intense light fields generated via a laser-driven relativistic plasma aperture. *Scientific reports*, 10(1):1–10, 2020.

[9] R. J. Gray et al. Enhanced laser-energy coupling to dense plasmas driven by recirculating electron currents. *New Journal of Physics*, 20(3):033021, 2018.

[10] M. D. Perry et al. Self-phase modulation in chirped-pulse amplification. *Optics letters*, 19(24):2149–2151, 1994.

[11] D. Milam. Review and assessment of measured values of the nonlinear refractive-index coefficient of fused silica. *Applied optics*, 37(3):546–550, 1998.